Abundance of giant mineral dust particles

Insights from measured emitted dust size distributions during the J-WADI campaign

Hannah Meyer, Andres Alastuey, Sylvain Dupont, Vicken Etyemezian, Jessica Girdwood, Cristina González-Flórez, Adolfo González-Romero, Tareq Hussein, Mark Irvine, Konrad Kandler, Peter Knippertz, Ottmar Möhler, George Nikolich, Xavier Querol, Chris Stopford, Franziska Vogel, Frederik Weis, Andreas Wieser, Carlos Pérez García-Pando, and Martina Klose

J-WADI (Jordan Wind erosion And Dust Investigation)

- One-month observation period in Jordan in Sep 2022.
- Goal: advance our understanding of **emitted dust properties**.
- Focus of this study:
  - Particle size distribution in the size range of particle diameters d_p between **0.4 and 200µm,**
  - **Super-coarse** ($10 \leq d_p < 62.5$ µm) and **giant particles** ($d_p > 62.5$ µm).

Mineral dust mass concentration PSD at J-WADI

- Significant mass concentration **dC_m abundance of particles d_p > 10 µm.**
- Mass concentration **peaks at up to d_p = 30 µm.**
- With increasing u_*, the mass concentration increases while the shape of the PSD remains similar.

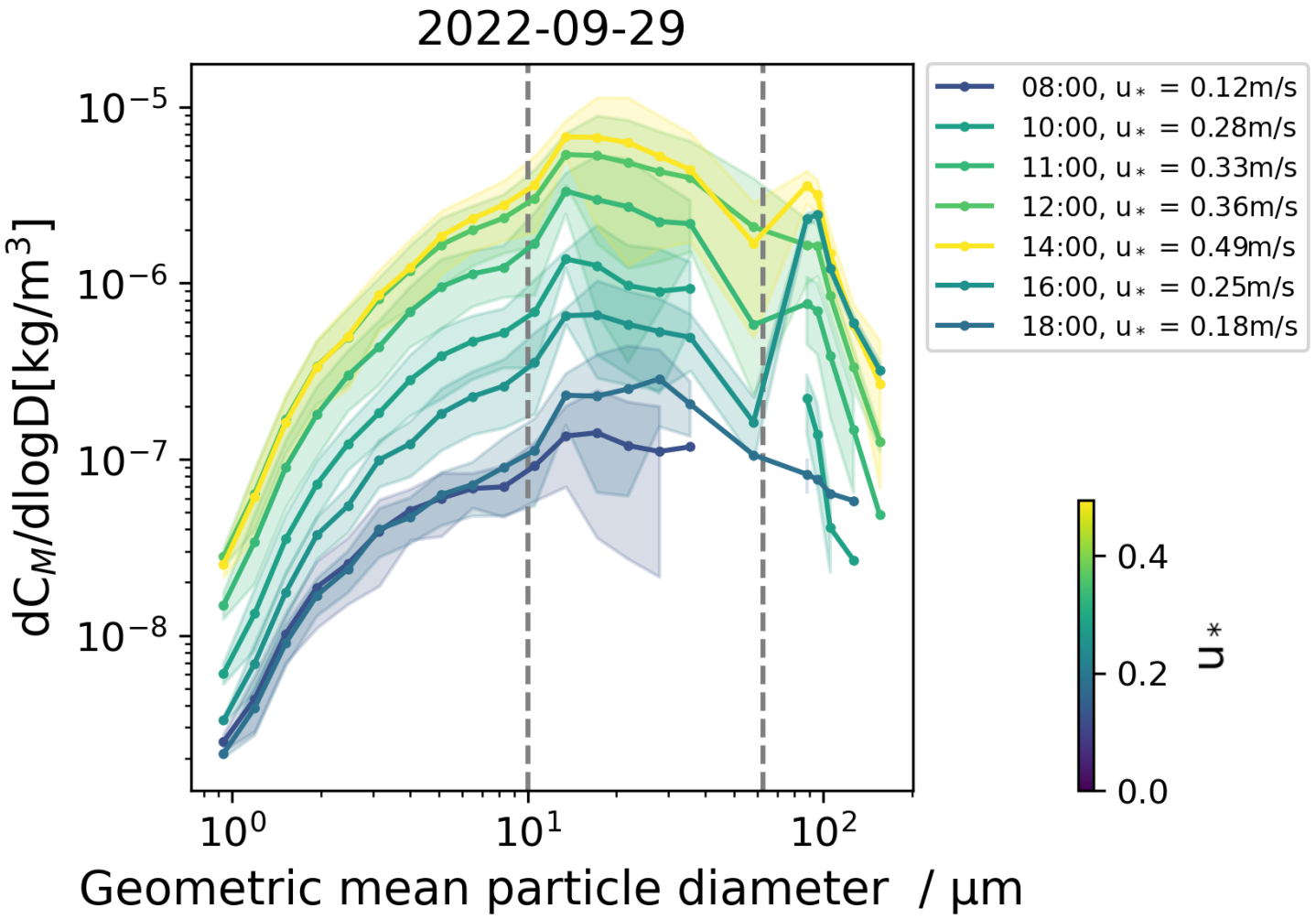

Abundance of giant mineral dust particles

Insights from measured emitted dust size distributions during the J-WADI campaign

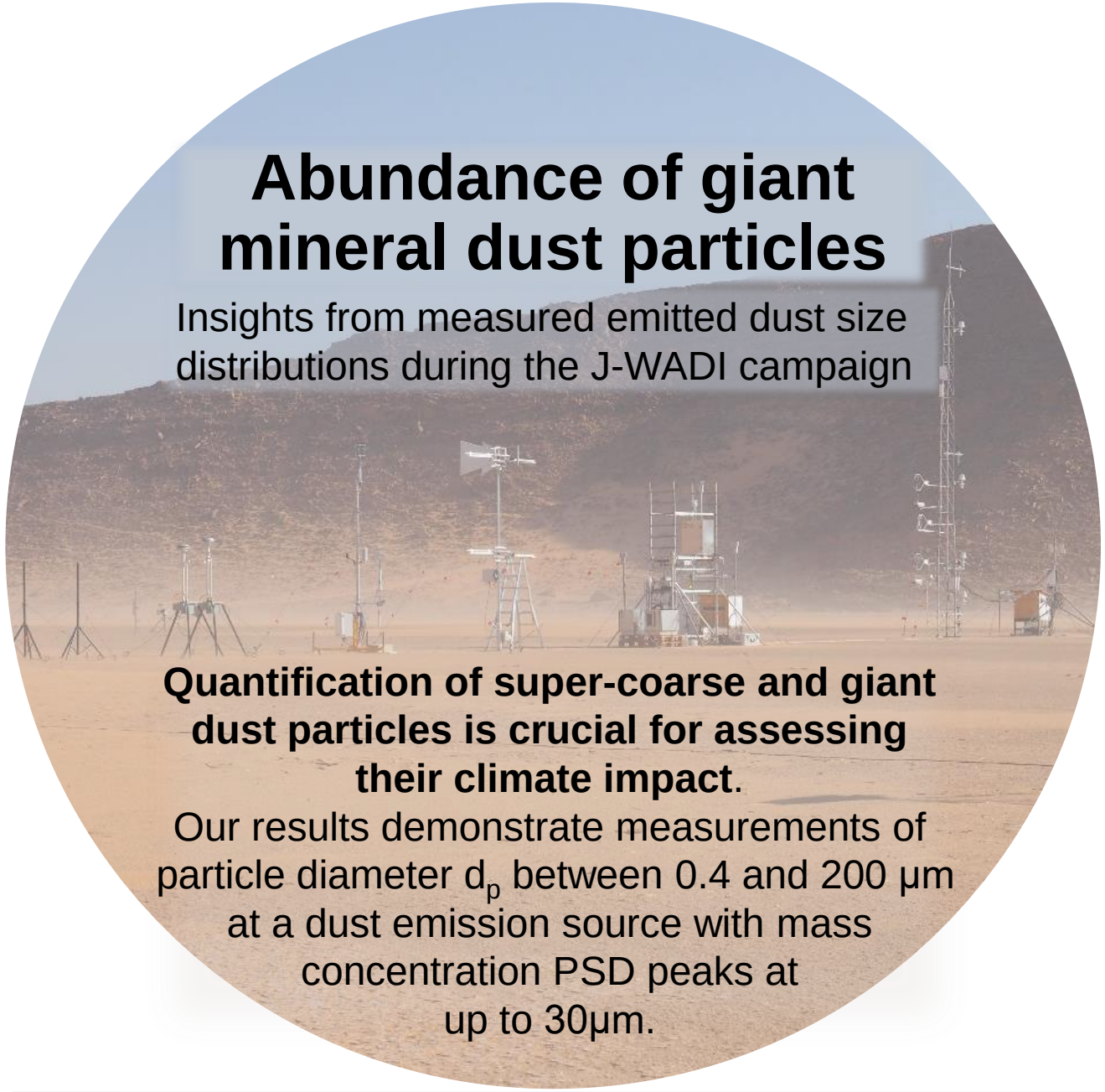

Quantification of super-coarse and giant dust particles is crucial for assessing their climate impact.
Our results demonstrate measurements of particle diameter d_p between 0.4 and 200 µm at a dust emission source with mass concentration PSD peaks at up to 30µm.

Karlsruhe Institute of Technology

- J-WADI campaign
- Aerosol spectrometers
- Results
- Inlet and systematic bias corrections

J-WADI (Jordan Wind erosion And Dust Investigation)

- Principal investigators and main organizers:
  Martina Klose (KIT) and
  Carlos Pérez Garcia-Pando (BSC)
- Sep 2022 at a dust source in Jordan
- Focus aspects:
  - emission and continued suspension of **super-coarse and giant dust particles**
  - variability of the emitted dust **particle-size distribution**
  - size-resolved **mineralogy** of dust at emission
  - **optical properties** of the emitted dust
  - **ice nucleation** by mineral dust

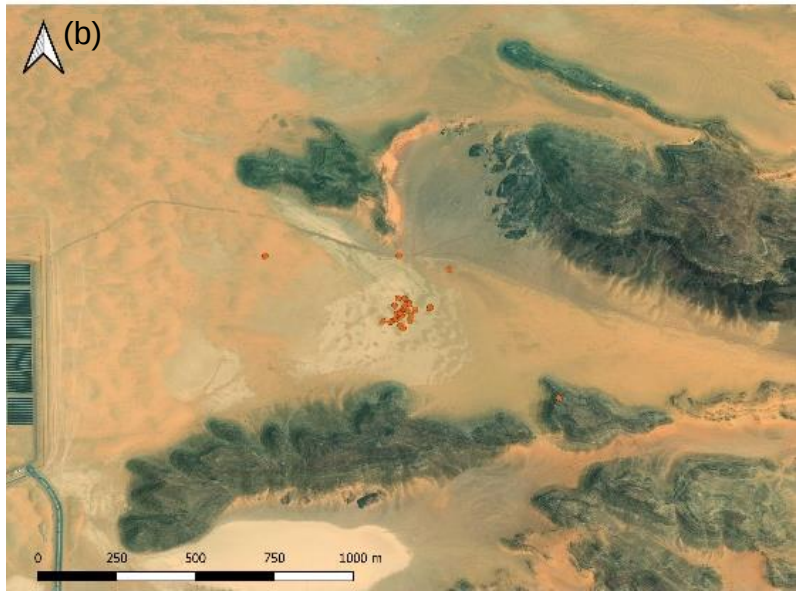

More information about J-WADI:

https://www.imk-tro.kit.edu/english/11800.php

Fig. 1: (a) Field location in Jordan, background image from Bing maps. (b) Field setup during J-WADI; background map copyright: Esri, Maxar, Earthstar Geographics, and the GIS User Community.

Aerosol spectrometers

- Several instruments of J-WADI cover **super-coarse** (10 µm ≤ d_p < 62.5 µm) and **giant particles** (d_p > 62.5 µm, Fig. 2a).
- Measurements are taken at 2 and 4 m height.
- On scaffolding (Fig. 2b):
  2 Fidas 200S and 2 Welas 2500
  (Palas GmbH, share air flow, directional inlet),
  1 CDA (Palas GmbH, Sigma-2 inlet).
- On rotating mast (Fig. 2c):
  4 SANTRI2
  (Desert Research Institute, 5 sensors per device, open-path),
  2 UCASS
  (University of Hertfordshire, nearly open-path).

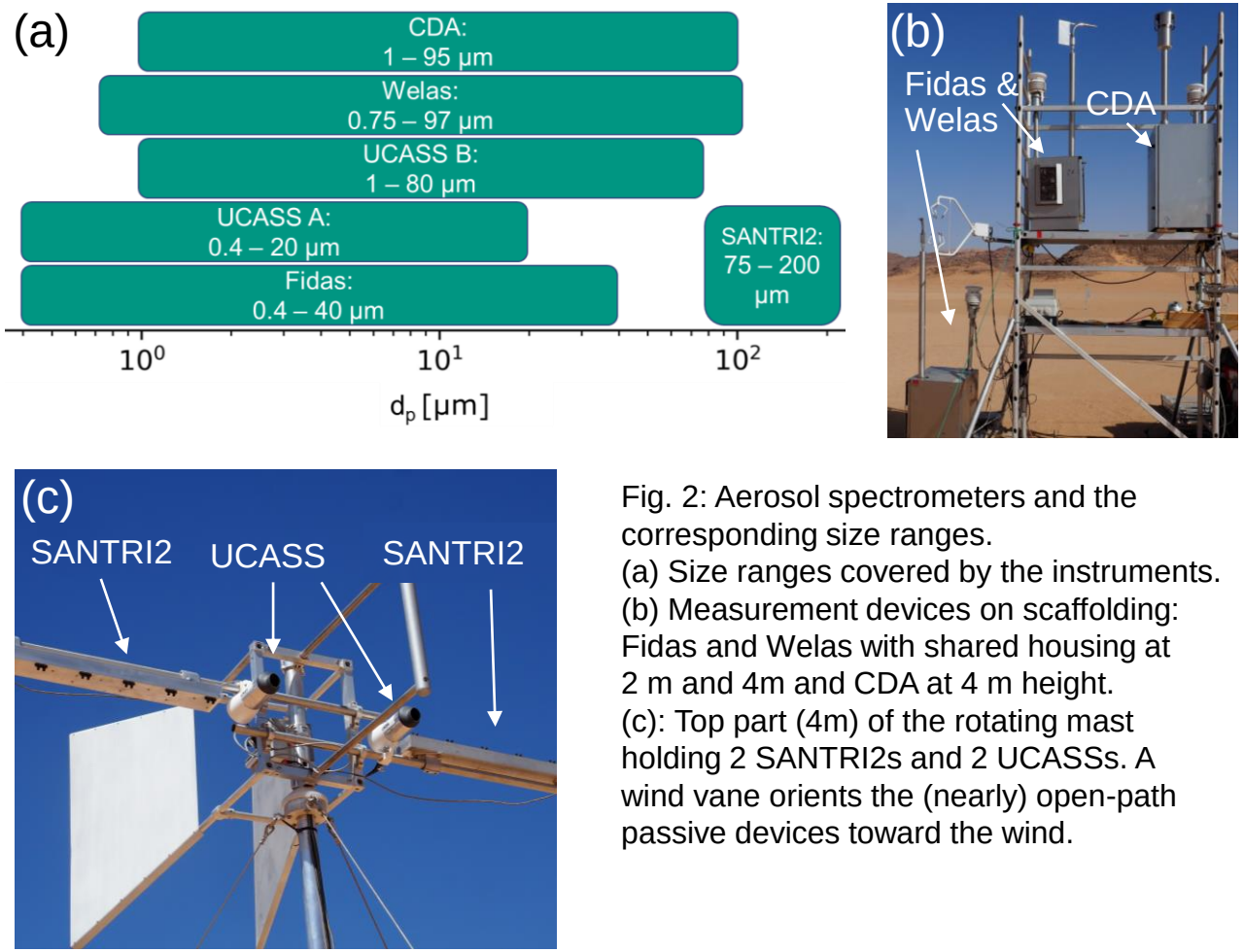

Fig. 2: Aerosol spectrometers and the corresponding size ranges.
(a) Size ranges covered by the instruments.
(b) Measurement devices on scaffolding: Fidas and Welas with shared housing at 2 m and 4m and CDA at 4 m height.
(c): Top part (4m) of the rotating mast holding 2 SANTRI2s and 2 UCASSs. A wind vane orients the (nearly) open-path passive devices toward the wind.

Campaign conditions

- High potential air temperature ($\theta_{Ødaily_{min}}$ = 25.4 °C, $\theta_{Ødaily_{max}}$ = 39.9 °C), low humidity ($RH_{Ødaily_{min}}$ = 20 %, $RH_{Ødaily_{max}}$ = 61 %), and no precipitation.
- Local dust emission typically during afternoons with wind speeds $v_{4m} \approx 6$ ms^{-1}.
- **Several events with high total mass concentrations** ($C_m > 10^4$ µgm^{-3}) were registered with d_p up to 70 µm (Fig. 3a).
- At friction velocities $u_* > 0.25$ms^{-1} a significant amount of particles > 10 µm is measured (u_*, Fig. 3b).
- Most continuous event on Sep 29th.

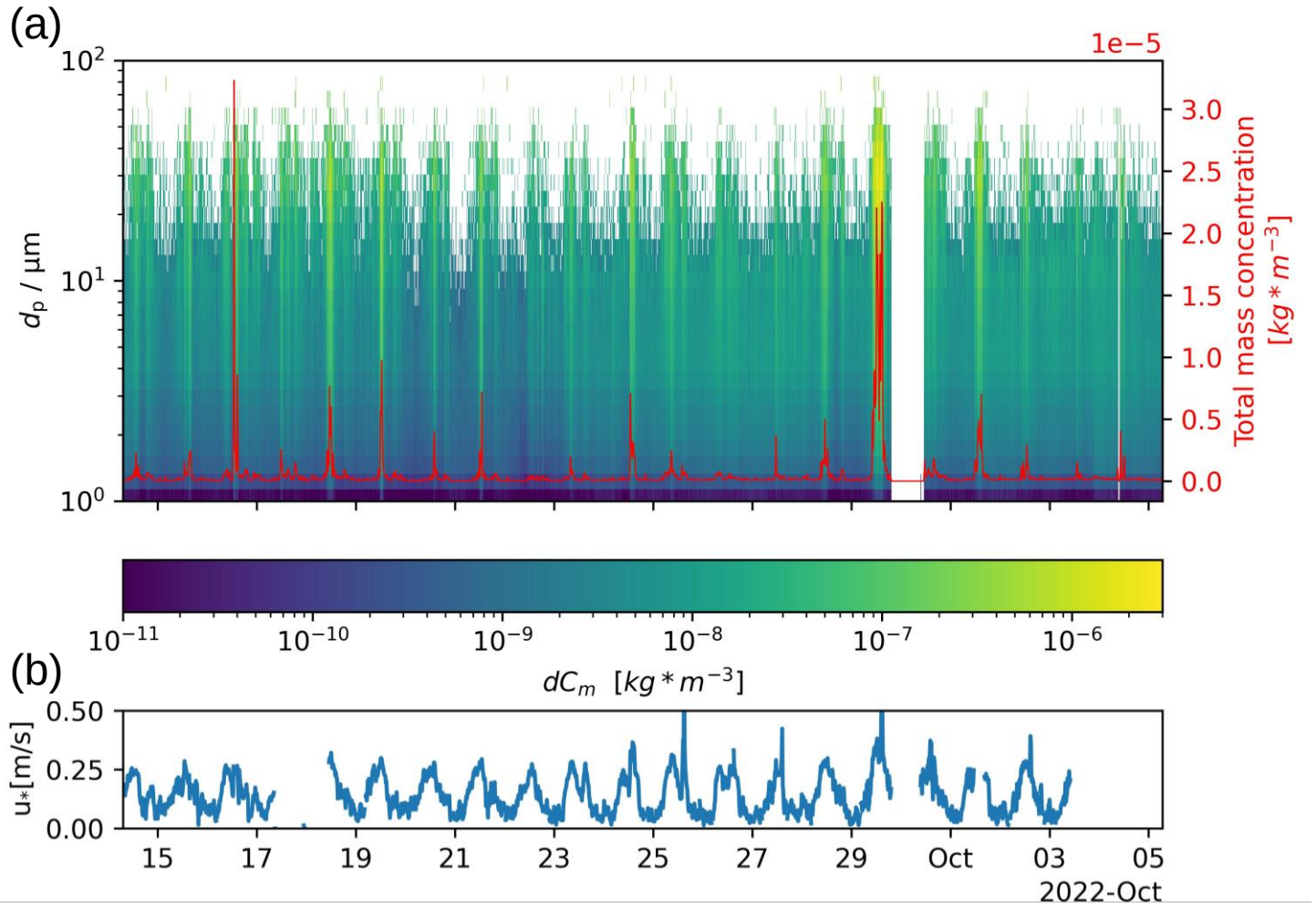

Fig. 3: (a) 1h averaged (total) mass concentration time series registered by Welas 4m. (b) Friction velocity u_* obtained by a scintillometer.

Particle size distribution (PSD) of Sep 29th

- Significant mass concentration **dC_m abundance of particles d_p > 10 µm registered with peaks at up to 30 µm** (Fig. 4).
- PSDs across instruments show considerable variability, particularly for d_p > 10 µm and regarding the position of the peak.
- Fidas and Welas show consistent PSDs for d_p < 7 µm, and CDA and Welas for d_p < 15 µm.
- UCASS A and B and Welas agree well.
- The SANTRI2s registered higher mass concentration PSDs than would be expected from the concentrations of the other instruments.

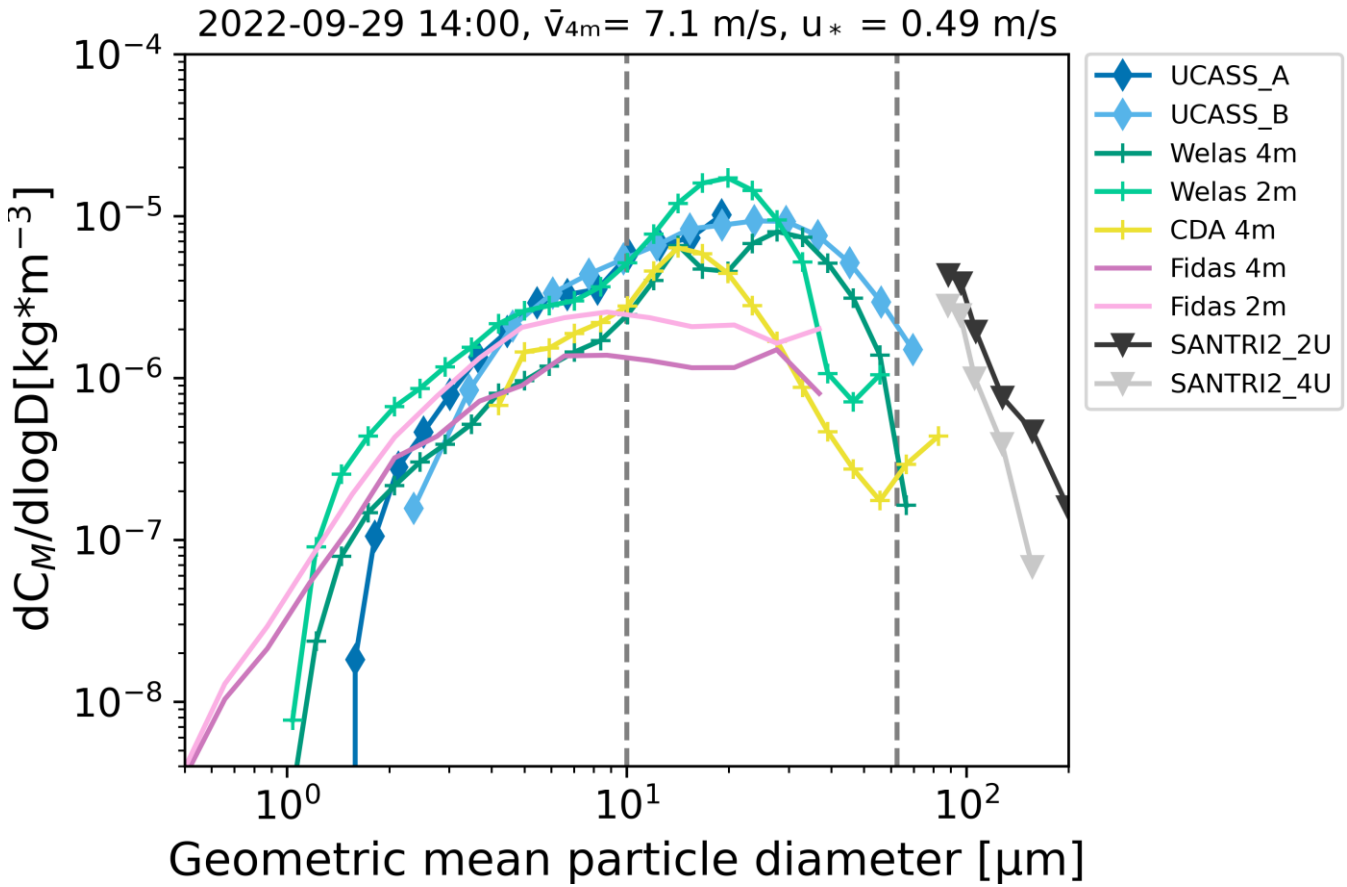

Fig. 4: 1 hour averages of size distributions by mass on 14 UTC Sep 29th.

Evolution of PSDs on Sep 29th

- Fig. 5 shows PSDs for varying wind conditions. The PSDs of different instruments differ in how well they fit together for different wind conditions.
- While UCASS A and B and Welas fit well together and Fidas and Welas show consistent PSDs for d_p < 7 µm, the position of the peak of different instruments varies between d_p ~10 µm and 40 µm.

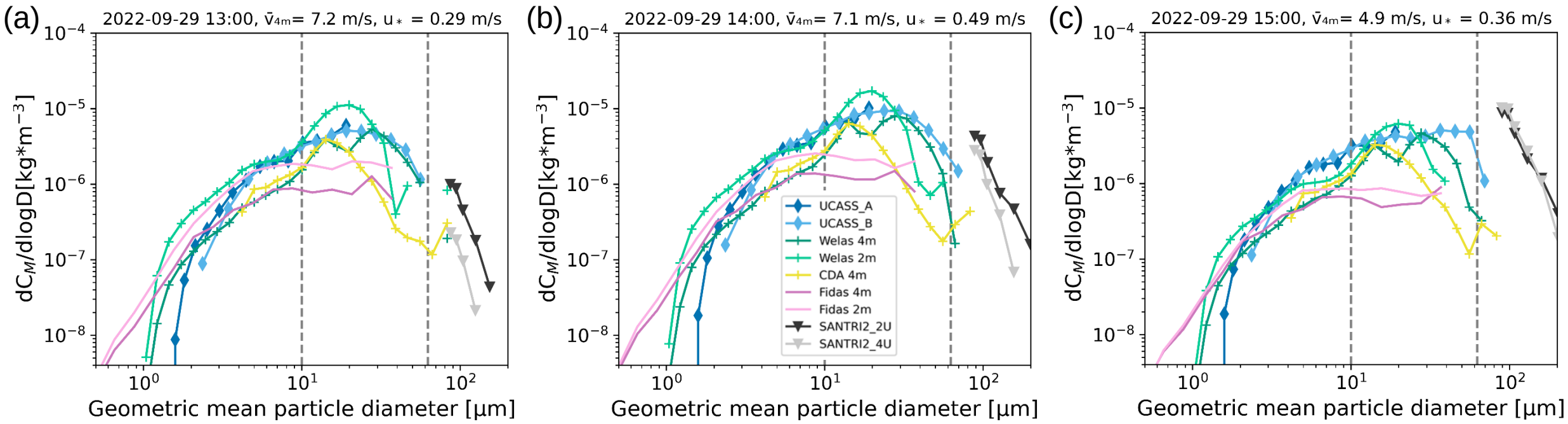

Fig. 5: 1 hour averages of PSD by mass on Sep 29th. (a) 13 UTC. (b) 14 UTC. (c) 15 UTC.

Variability of PSDs on Sep 29th

- Fig. 6 shows the variability of all instruments averaged 1 hour mass size distributions with time and u* on Sep 29th.
- With **increasing u_*, the mass concentration increases** (as expected) while the shape of the PSD stays similar. However, the PSD with the largest u_* of Sep 29th shows little difference to that corresponding to the second largest u_*.

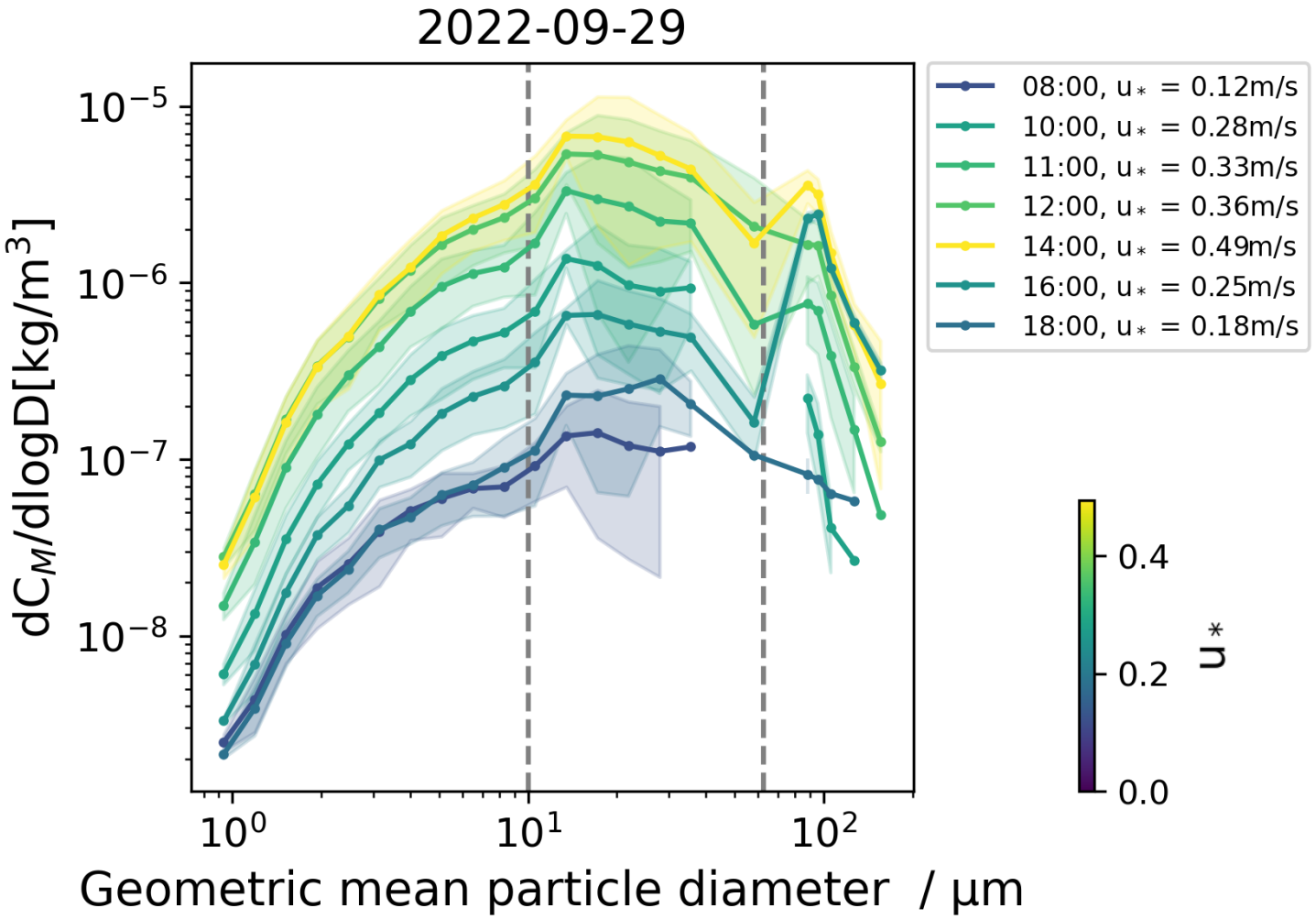

Fig. 6: All instruments 1h averaged mass size distribution on Sep 29th. Shaded areas indicate the standard deviation of all instruments. Colors indicate u_*.

Particle size distribution of the whole campaign

- Fig. 7a shows the variability of all instruments 1 hour averaged mass concentration PSDs with u_* during the whole measurement period. The higher u* the higher dC_M (as expected).
- As u_* increases, more large particles are measured with **most abundant super-coarse particles with high u_* at d_p between 10 and 30 µm.** Above ~30 µm for increasing u_* dC_M either decreases or increases (Fig. 7b).

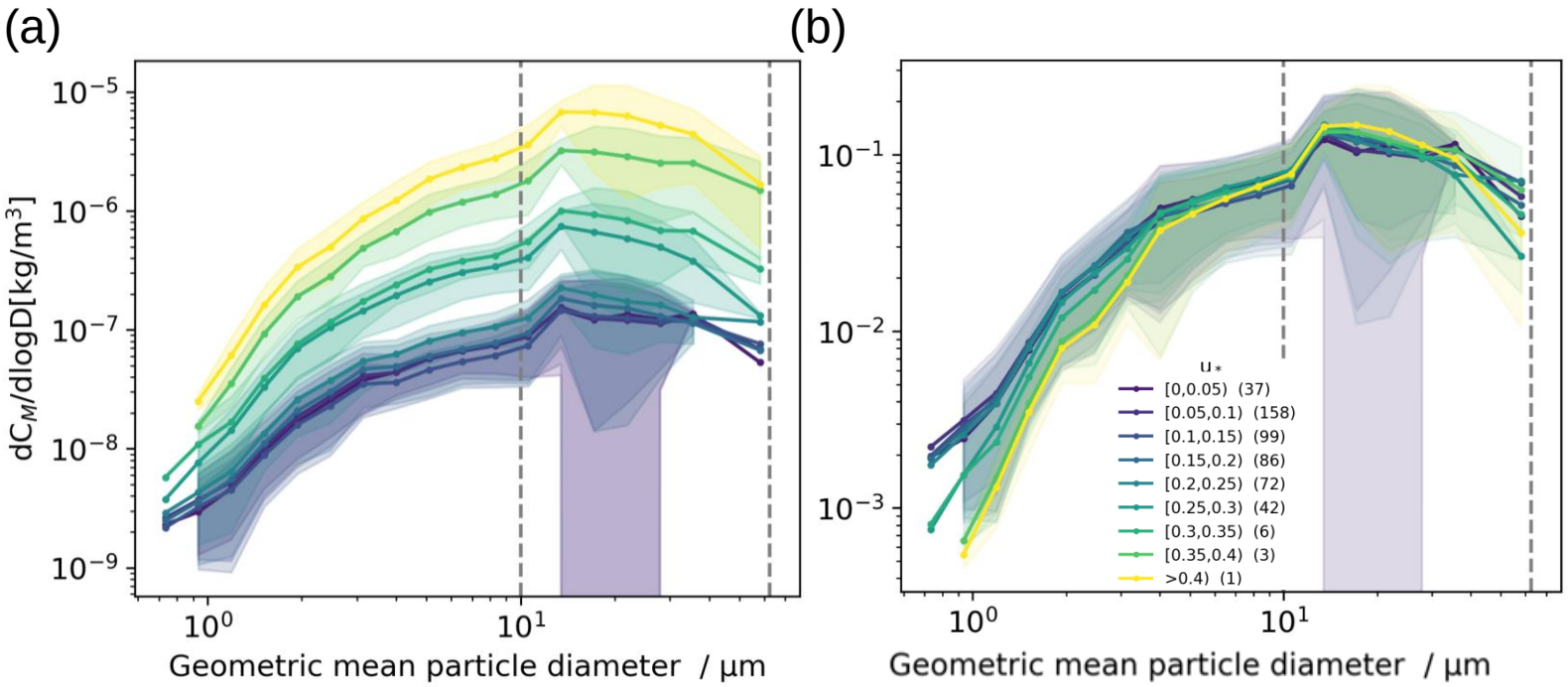

Fig. 7: All instruments 1h averaged mass concentration PSDs. Shaded areas indicate the standard deviation across instruments. (a) non-normalized. (b) normalized

Intercomparison correction

- To identify and rectify any **systematic biases** among the instruments, we implemented an **intercomparison period** at the end of the campaign in which **all instrument types were operated at the same height** (SANTRI2 on the ground for enhanced counting statistics, others at 2 m, Fig. 8a).
- We utilized the **intercomparison data to calibrate** the measurements using the linear regression's slope between the instruments [1], (Fig. 8b).

(a)

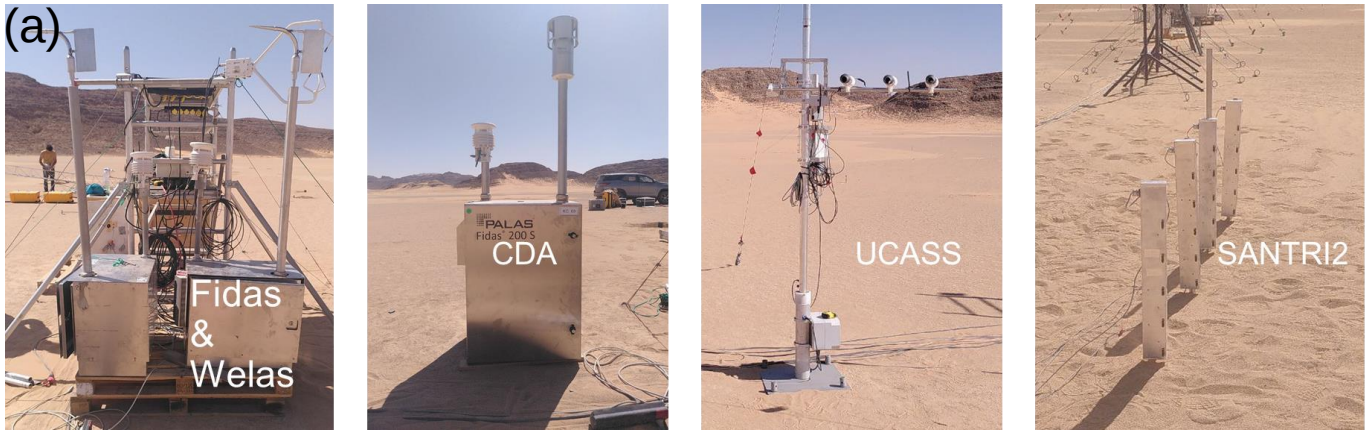

(b)

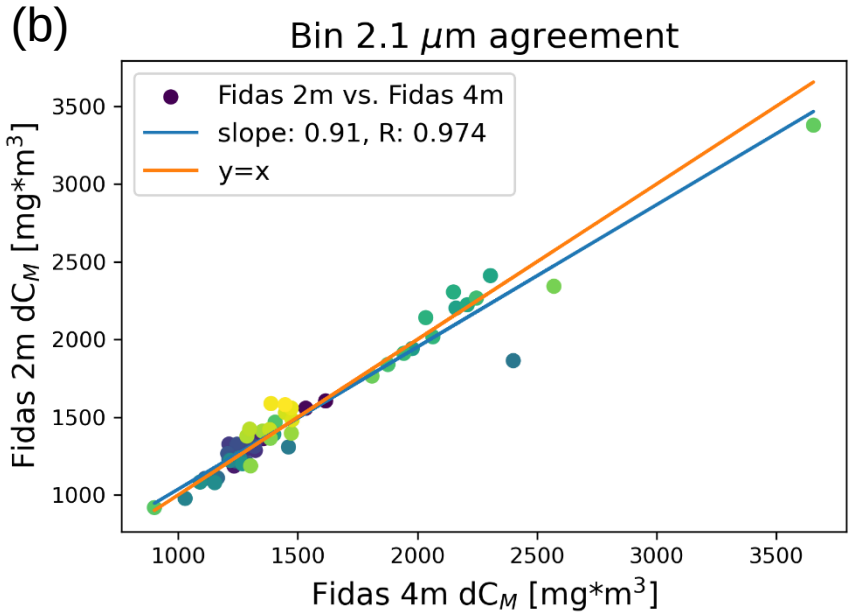

Fig. 8: (a) All instruments used for the study in intercomparison set-up. (b) Example of linear regression for the correction applied to a bin (2.1 µm) of the Fidas instruments. Fidas 2m serves as the reference, while Fidas 4m is adjusted by the slope determined from the linear regression. At correlations lower than 0.6, no correction was applied. Similar procedures were conducted with Welas 2m/Welas 4m, Welas 2m/CDA, SANTRI2_2U/SANTRI2_4U, and all averaged instruments/UCASS A (reference/to be corrected, respectively).
[1] González-Flórez et al. (2023), https://doi.org/10.5194/acp-23-7177-2023.

Sampling efficiency

- The sampling efficiency η depends on inlet/pipe design, flow dynamics, and particle characteristics.
- UCASS, Fidas & Welas, and CDA inlets exhibit **varied sampling efficiencies η.**
- **Fidas and Welas inlets were characterized** using empirical models [1,2], (Fig. 9a). For wind speeds v ≤ 5 ms^{-1} and diameters d_p ≤ 5 µm, the efficiency η ≈ 100 % and decreases to 0 % at d_p ≈ 30 µm. For v > 5 ms^{-1} and d_p > 5 µm, η increases peaking at d_p ≈ 12 µm and decreases to 0 % at d_p ≈ 40 µm.
- By dividing the mass concentration PSDs of Fidas and Welas by the sampling efficiencies η of the directional inlet, corrected PSDs can be estimated (Fig. 9b). These results may be unrealistic and require further evaluation.

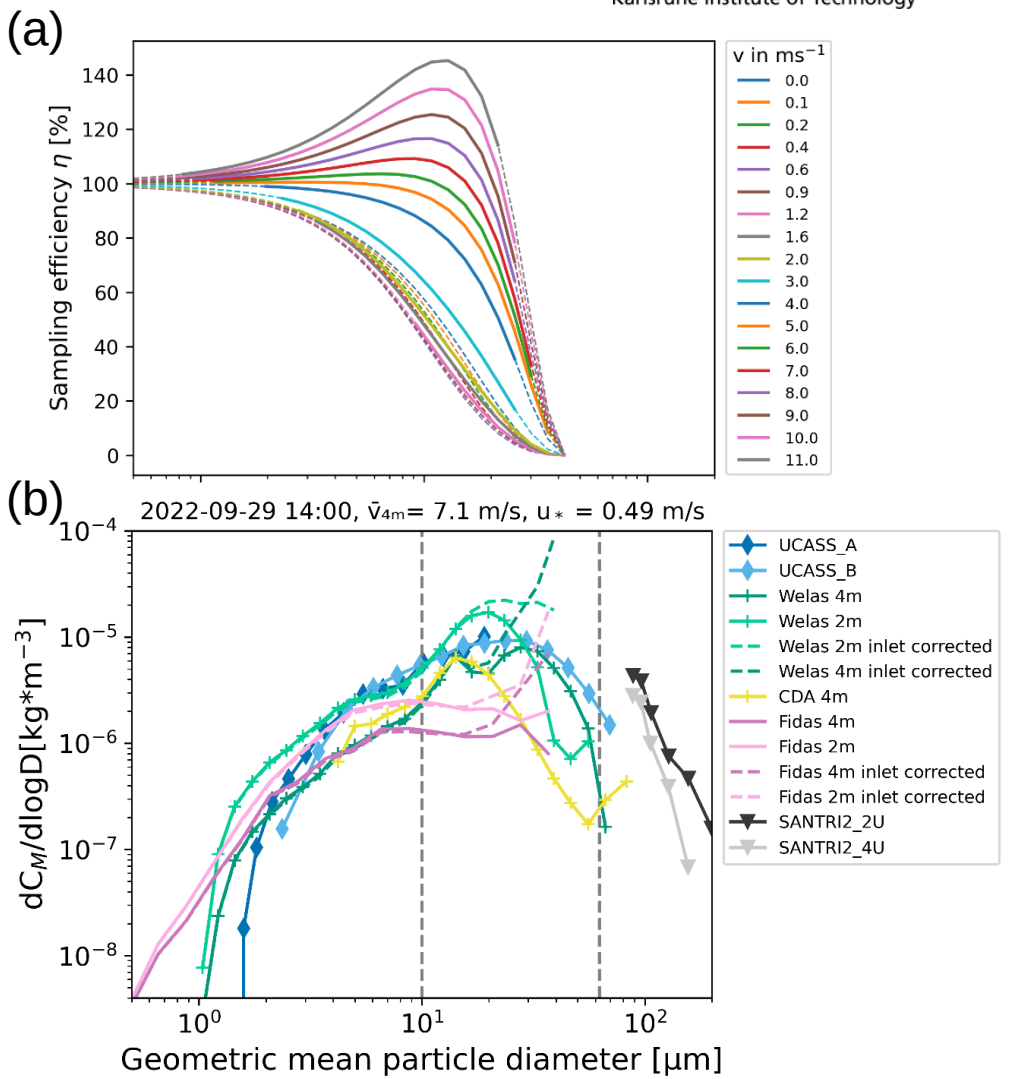

Fig. 9: (a) Sampling efficiency of Fidas & Welas for different wind speeds.
(b) Mass concentration PSDs with directional inlet.
[1] Willeke, K. and Baron, P. (2005), doi:10.1002/9781118001684.
[2] Zhang et al. (2012), https://doi.org/10.1016/j.jaerosci.2012.05.007.

hannah.meyer@kit.edu

Conclusion: Abundance of giant mineral dust particles

- The PSD in the **diameter range between 0.4 and 200 µm** was measured during J-WADI.
- Super-coarse particles were abundant, giant particles were detected.
- **Peak at up to 30 µm in mass concentration PSD.**
- The efficiency of the directional inlet was calculated and corrected but needs to be further evaluated.
- Future research will focus on:
  - further understanding the variability of different aerosol spectrometers,
  - analyzing mechanisms driving the emission and transport of super-coarse and giant dust particles.

We thank…

- …all project partners and the whole J-WADI team.
- … A. Böhmländer, B. Deny, T. Gamer, M. Gonçalves Ageitos, L. Ilic, R. Miller, S. Scheer, R. Sousse Villa, and S. Vergara Palacio for their support during campaign preparation and implementation.
- …for the funding: J-WADI was funded through the Helmholtz Association's Initiative and Networking Fund (grant no. VH-NG-1533), which primarily funded the work presented here, and the European Research Council under the Horizon 2020 research and innovation programme through the ERC Consolidator Grant FRAGMENT (grant no. 773051).
- ...you for your attention.

hannah.meyer@kit.edu